European Polymer Journal 241 (2025) 114373

Contents lists available at ScienceDirect

European Polymer Journal

journal homepage: www.elsevier.com/locate/europolj

Sulfur-containing polyesters from thioanhydride/CS_2/epoxide ring-opening terpolymerisation: monomer scope and gold-nanoparticle functionalisation☆

Cesare Gallizioli [a], Marina Sebastian [b,c], Malte Cornelsen [a], Christian Rossner [b,c,d,*], Alex J. Plajer [a,e,*]

[a] Makromolekulare Chemie, Universität Bayreuth, Universitätsstraße 30, 95447 Bayreuth, Germany
[b] Leibniz-Institut für Polymerforschung Dresden e.V., D-01069 Dresden, Germany
[c] Faculty of Chemistry and Food Chemistry, Technische Universität Dresden D-01069 Dresden, Germany
[d] Department of Polymers, University of Chemistry and Technology Prague, Technická 5, Prague 6 166 28, Czech Republic
[e] Bayrisches Polymer Institut (BPI), Universität Bayreuth, Universitätsstraße 30, 95447 Bayreuth, Germany

A B S T R A C T

Sulfur-containing polymers are receiving increasing attention due to their unique material and chemical properties, yet access to functional variants remains limited. To address this challenge, the ring-opening terpolymerisation (ROTERP) of phthalic thioanhydride (PTA), carbon disulfide (CS_2), and a range of substituted epoxides was investigated. Polymerisation of linear, branched, aromatic, fluorinated, ether-functionalized, and multi-functional epoxides was achieved, thus providing access to a versatile range of sulfur-rich polymers bearing trithiocarbonate functionalities. Most systems exhibited moderate to high sequence selectivity for an alternating poly(ester-alt-ester-alt-trithiocarbonate) terpolymer structure, with some incorporation of polymer links from the competing ring-opening copolymerisation (ROCOP). The materials demonstrated moderate thermal stability under nitrogen ($T_{d,5\%}$ up to 314 °C) and tunable glass transition temperatures (T_g ranging from −20 to 163 °C). The trithiocarbonate groups incorporated along the main chain were employed for grafting the polymer chains to gold nanoparticle surfaces, yielding colloidally stable agglomerates. Furthermore, aldehyde-bearing polymers enabled attachment of organic moieties to the polymer grafted-to the nanoparticles via imine condensation, which could be selectively released under acidic conditions. Our study demonstrates the power of ROTERP as a synthetic platform to access a broad catalogue of functional sulfur-containing polymers and nanomaterials from readily available epoxides.

1. Introduction

Sulfur-containing polymers offer distinct properties compared to their all-oxygen analogues [1–7]. These include the ability to coordinate metals, enhanced semi-crystallinity, improved depolymerisability, and superior optical properties. Following early synthetic efforts via polycondensation reactions, various methodologies have recently emerged that offer improved synthetic control. Among these, ring-opening polymerization (ROP) of heterocycles — such as thiolactones, thioesters, and thiiranes — yields homopolymers, including polythioesters, polythiocarbonates, and polythioethers (see Fig. 1(a)) [8–13]. In some cases, the ROP of three- or four-membered heterocycles can be coupled with the insertion of heteroallenes or cyclic anhydrides to generate alternating copolymers, in a process known as ring-opening copolymerization (ROCOP). Sulfur-containing examples include carbon disulfide/epoxide ROCOP to form poly(thiocarbonates) and cyclic thioanhydride/epoxide ROCOP to produce poly(ester-*alt*-thioester)s (see Fig. 1(b)) [14–30]. Recently, we demonstrated alternating ring-opening terpolymerization (ROTERP) of ternary monomer mixtures comprising phthalic thioanhydride (PTA), CS_2, and propylene oxide (PO). Using a simple lithium catalyst—such as lithium benzyloxide (LiOBn)—this process selectively forms poly(ester-*alt*-ester-*alt*-trithiocarbonates) with up to 98 % selectivity, rather than the competing poly(ester-*alt*-thioester) formation from PTA/PO ROCOP (see Fig. 1(c)) [31–33]. However, particularly at lower catalyst loadings, PTA/PO ROCOP is also observed, leading to a more irregular microstructure [34–38]. The poly(ester-*alt*-ester-*alt*-trithiocarbonate) links exhibit an unusual regio selectivity, with ester groups adjacent to tertiary carbon centres and trithiocarbonates adjacent to secondary carbon centres [39]. Despite this, the epoxide scope remained limited, and no further applications of these polymers had been investigated. Building on this, the motivation of this work was twofold: Firstly, we identified a series of

☆ This article is part of a special issue entitled: 'P- and S-containing polymers' published in European Polymer Journal.

* Corresponding authors.
E-mail addresses: rossner@ipfdd.de (C. Rossner), alex.plajer@uni-bayreuth.de (A.J. Plajer).

https://doi.org/10.1016/j.eurpolymj.2025.114373
Received 24 September 2025; Received in revised form 27 October 2025; Accepted 29 October 2025
Available online 1 November 2025

other monomer combinations that undergo ROTERP [40–42]. We hypothesized that PTA/CS_2/epoxide ROTERP should, in principle, provide straightforward access to a wide range of sulfur-containing polymers, leveraging the many epoxides developed for epoxide ROP [43–45]. In testing this hypothesis, we demonstrate that a broad variety of polymer structures—with tuneable thermal properties and functionalities—are easily accessible via ROTERP. Secondly, we aimed to make use of the dual functionality of trithiocarbonate moieties incorporated in the polymer backbone on one hand and additional functional groups that are introduced with the oxirane monomer on the other for the formation of hybrid nanomaterials. We hypothesized that the trithiocarbonate groups enable straightforward anchorage of the synthesized polymer molecules to gold nanoparticle surfaces (Fig. 1(d)), while aldehyde groups in the oxirane monomer would offer the possibility for dynamic covalent chemistry, enabling the controlled release of a cargo from the nanoparticulate support. Acid-promoted release of an organic dye from the colloidal gold species and concomitant restoration of its fluorescence served as a model scenario to test this possibility in this promising type of hybrid nanomaterials proving that ROTERP polymers can be applied in the functionalization of gold nanoparticles.

2. Results and discussion

To investigate whether PTA/CS_2/epoxide ROTERP is compatible with different epoxides and how sequence selectivity and polymer properties are affected, we employed a range of epoxides (see Fig. 2) under unified ROTERP conditions. For baseline comparison, butylene oxide (BO) and propylene oxide (PO)—used in our previous study—were also examined, albeit under different loading than previously investigated [31].

Performing CS_2/PTA/BO ROTERP (Table 1, run #1) using 1 eq. lithium benzyloxide (LiOBn, generated in situ from Li[$N(SiMe_3)_2$] and BnOH), 500 eq. BO, 200 eq. PTA, and 500 eq. CS_2 at 80 °C for 2 h resulted in 70 % PTA conversion. The polymer was isolated via precipitation from DCM/MeOH, and its microstructure, apparent molar mass and molar-mass distribution, and the thermal properties were evaluated (Fig. 3). The ^{1}H NMR spectrum (Fig. 3(a)) confirms that the polymeric product consists primarily of poly(ester-*alt*-ester-*alt*-trithiocarbonate) links from the ROTERP process. These are indicated by two aryl CH resonances from a symmetrically substituted aromatic unit at 7.60 and 7.45 ppm, connected to the tertiary CH at 5.27 ppm; the CH_2 group appears between 3.60 and 3.85 ppm. The CH resonance correlates to quaternary aryl ester signals at 133 ppm in the ^{1}H–^{13}C HMBC, while the CH_2 resonances correlate to trithiocarbonate groups (see ESI Figure S 8). Additionally, the ^{1}H NMR spectrum reveals the presence of thioester groups from co-occurring ROCOP, visible as minor aryl signals from unsymmetrically substituted aromatic units and CH_2 resonances at 3.01 ppm, which correlate to quaternary thioester resonances at 191 ppm in the ^{1}H–^{13}C HMBC spectrum. The sequence selectivity of the ROTERP process versus co-occurring ROCOP, as determined per ^{1}H NMR (see ESI Section S2), is 86 %. The estimated uncertainty of these values is ±5 % based on repeated integrations of independent spectra and signal overlap, as common for NMR methods.

Fig. 4(a) illustrates the proposed propagation mechanism for

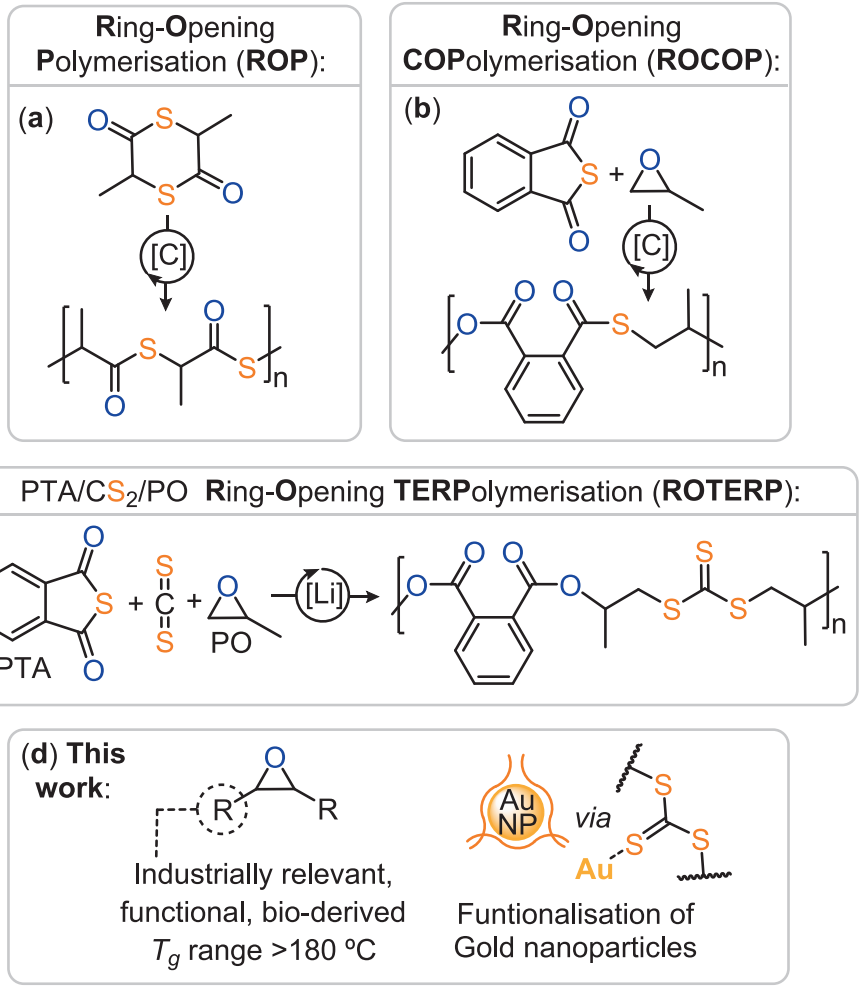

Fig. 1. Comparison of sulfur containing (a) ROP, (b) ROCOP and (c) ROTERP. (d) Outline of the current study.

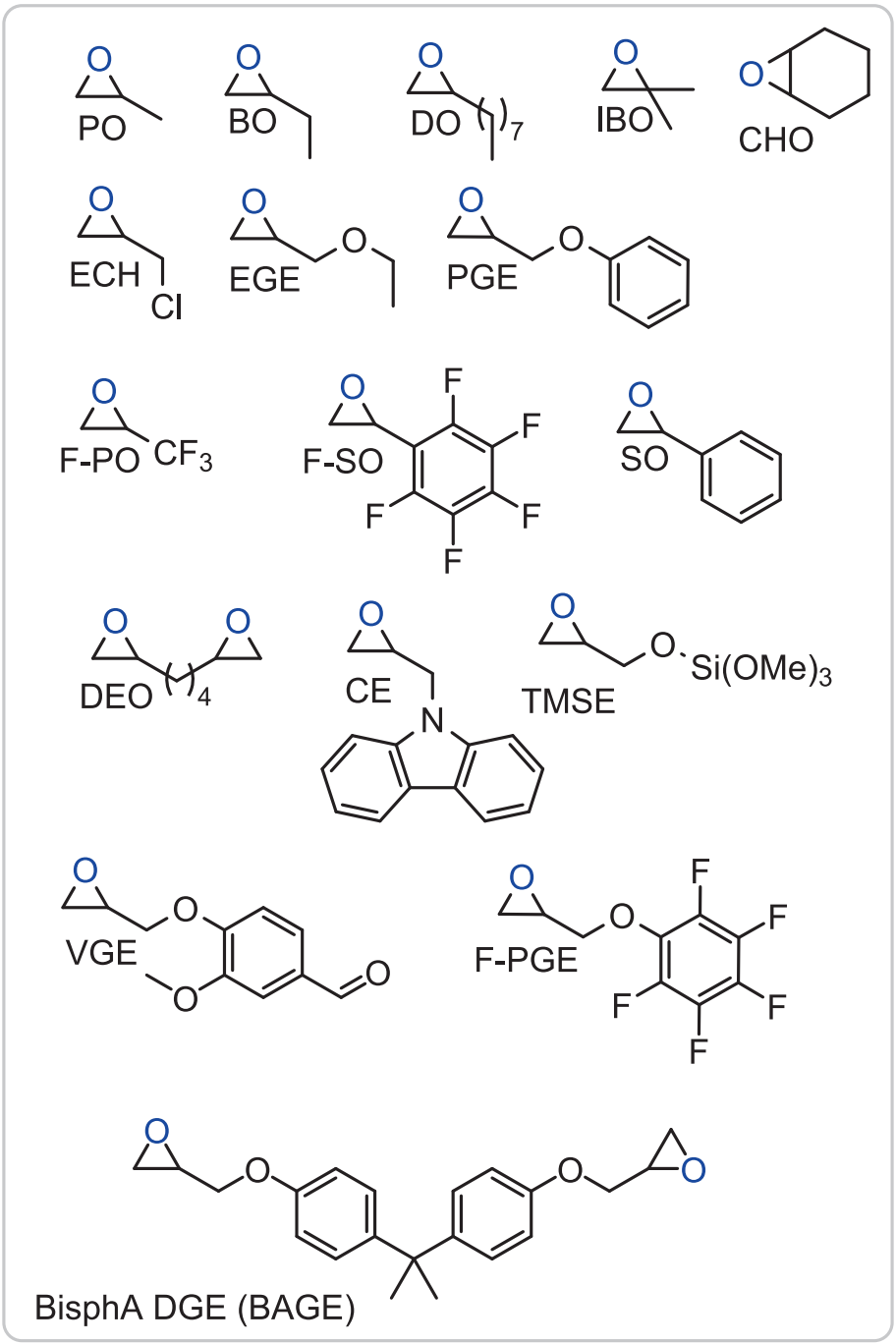

Fig. 2. Epoxides employed in this study.

ROTERP, while Fig. 4(b) shows the competing ROCOP pathway. Minor amounts (2 % relative to epoxide consumption) of cyclic dithiocarbonate by-products were also detected, consistent with the side pathway illustrated in Fig. 4(c).

Gel permeation chromatography (GPC) analysis of the polymer reveals an apparent weight-averaged molar mass of M_w = 58 kg/mol (polystyrene calibration) and a polydispersity of $Đ$ = 1.8. This polydispersity is well above the expected value for a controlled chain-growth polymerization, and accordingly, the molecular weight distribution is unsymmetric. This suggests the occurrence of side reactions such as chain transfer, chain-end coupling, and transesterification, which are commonly observed during sulfur-containing ROCOP [14]. Previous investigations on PTA/CS_2/epoxide ROTERP revealed that the polydispersities remained comparatively broad regardless of concentration, catalyst loading, or temperature [31]. Although the molecular weight increased linearly with conversion, resulting in some weight control, the polydispersity broadened with conversion. For a detailed mechanistic analysis, the reader is referred to our original contributions [31–33].

Differential scanning calorimetry (DSC) shows the material is amorphous, with a glass transition temperature (T_g) of 20 °C. Thermogravimetric analysis reveals a decomposition onset temperature ($T_{d,5\%}$) of 236 °C. These results serve as a reference for the other epoxides investigated.

Switching to epoxides with other aliphatic chains (Table 1, runs #2 and #3) significantly affects thermal properties. Moving from PO to BO and decyl oxide (DO) leads to a decrease in T_g to 20 °C and –20 °C, respectively. As expected, sequence selectivity and molar masses (normalized to conversion) remain comparable due to the chemical

Table 1
Polymerizations investigated in this study.

Run[a]	Epoxide	time	Conv. [%][b]	Polymer select. [%][c]	Sequence select. [%][d]	M_w [kg/mol][d]	$Đ$[d]	T_g [°C][e]	$T_{d(5\%)}$ [°C][f]
#1	BO	3 h	70	98	86	58	1.8	20	236
#2	PO	2 h	86	95	87	80	2.1	48	230
#3	DO	19 h	78	97	83	64	2	−20	258
#4	IBO	18 h	82	79	94	58	1.8	23	209
#5	CHO	72 h	20	96	75	7	1.8	115	233
#6	SO[g]	336 h	30	85	n. d.	3	1.5	37	211
#7	PGE	20 h	99	79	84	25	1.9	37	250
#8	EGE	25 h	92	97	79	26	1.6	9	241
#9	ECH	15 h	90	92	91	24	1.9	54	209
#10	TMSE[h]	45 min	84	89	88	n. d.	n. d.	−15	255
#11	VGE	22 h	82	92	53	11	1.7	81	256
#12	CE[g]	16 h	75	70	n. d.	35	1.3	136	269
#13	F-PO	20 h	88	56	91	25	1.6	62	314
#14	F-PGE	5 h	83	93	87	43	1.2	40	255
#15	F-SO[g]	384 h	40	90	n. d.	7	1.3	90	249

[a] ROTERP conducted at 80 °C and with a loading of 1 eq. LiOBn: 500 eq Epoxide: 200 eq. PTA: 500 eq. CS_2.
[b] Relative peak integrals of aromatic signals in the normalised ^{1}H NMR spectrum ($CDCl_3$, 400 MHz) of the crude reaction mixture corresponding to polymer resonances.
[c] Relative peak integrals of the CH signals in the normalised ^{1}H NMR spectrum ($CDCl_3$, 400 MHz) of the crude reaction mixture corresponding to polymer resonances.
[d] Relative peak integrals of the CH_2 signals in the normalised ^{1}H NMR spectrum ($CDCl_3$, 400 MHz) of polymer resonances corresponding to ROTERP links. [d]Determined by GPC (gel permeation chromatography) measurements conducted in THF on a system calibrated using narrowly dispersed polystyrene standards.
[e] Determined by differential scanning calorimetry (DSC) from a second heating curve at 10 K/min.
[f] Determined by thermogravimetric analysis (TGA).
[g] Complete determination of selectivity not possible due to overlapping signals.
[h] Cross-linking from hydrolysis of −Si(OMe)$_3$ groups preventing GPC.

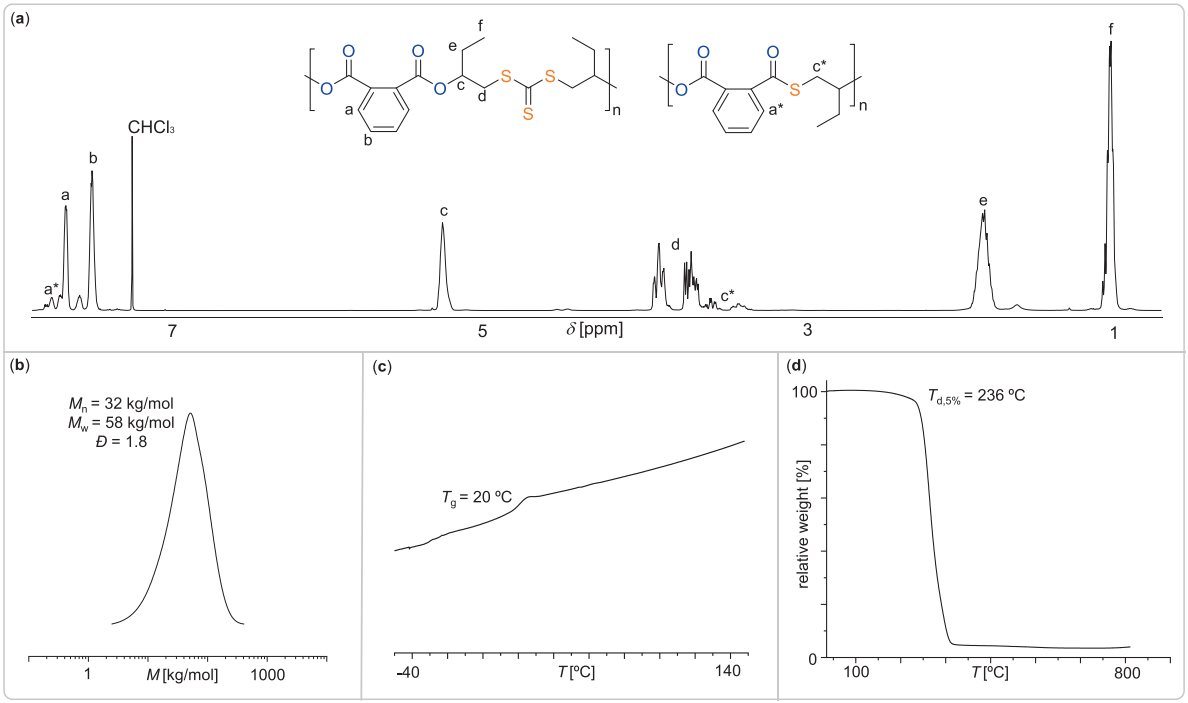

Fig. 3. (a) ^{1}H NMR (b) GPC, (c) DSC and (d) TGA data of precipitated polymer corresponding to table 1 run #1.

similarity of the monomers.

We next explored disubstituted epoxides, focusing on 1,2-dimethyl epoxide (isobutylene oxide, IBO; run #4). Under analogous conditions, ROTERP yielded 82 % PTA conversion after 18 h, affording a polymer with 94 % sequence selectivity—higher than its monosubstituted counterpart, PO. According to the ROTERP mechanism (Fig. 3), this suggests that the alkoxide intermediate formed from IBO ring-opening facilitates O/S exchange via back-biting, consistent with prior reports in sulfur-containing ROCOP [17]. However, increased formation of cyclic dithiocarbonate by-products reduced overall polymer selectivity to 79 %. GPC analysis shows Mw = 58 kg/mol ($Đ$ = 1.8). As the epoxide contains no stereocenter, which could render the resulting polymer atactic, it shows a semi-crystalline behavior with a T_g of 23 °C, melting temperature T_m of 110 °C (see ESI Figure S 23), similar to recent polymers obtained from IBO, and a thermal decomposition onset at 209 °C [46].

Cyclohexene oxide (CHO, run #5) was also included in the monomer scope due to its potential to yield polymers with improved thermal

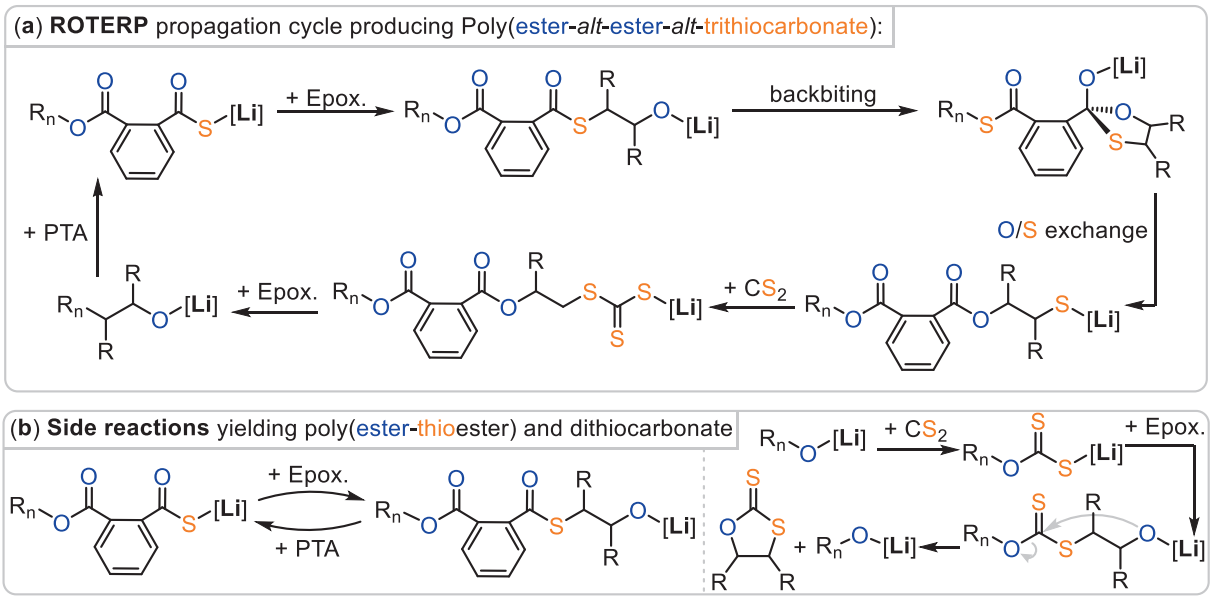

Fig. 4. (a) PTA/CS_2/Epoxide ROTERP propagation mechanism. During each cycle, the degree of polymerization indicated by the subscript *n* increases. (b) Co-occurring side reactions.

properties, owing to its bicyclic structure. Consistent with this, ROTERP with CHO gave a high T_g of 115 °C and a decomposition onset at 233 °C. However, the polymerization efficiency was notably reduced, achieving only 20 % PTA conversion after 72 h. GPC confirms the formation of shorter polymers (M_w = 7 kg/mol, $Đ$ = 1.8), potentially due to a higher concentration of diol impurities—an often-encountered issue with CHO in ROCOP [47]. Attempts to obtain higher weight materials by adapting the loading failed, which implies some limitation of the ROTERP process. Sequence selectivity also dropped to 75 %, presumably due to steric hindrance from the rigid cyclohexyl ring interfering with O/S exchange via backbiting.

Next, we turned to styrene oxide (SO, entry #6), a challenging epoxide in ROCOP. Due to SO's aromatic substituent rendering the CH position more prone to nucleophilic attack, ring-opening typically occurs at both the CH_2 and CH positions, resulting in a loss of regioselectivity [48]. In our case, slow polymerization occurred, reaching only 30 % PTA conversion after 14 days. ^{1}H NMR spectroscopy confirms regio-unselective polymerization, showing multiple broad and overlapping resonances. Due to this lack of regioselectivity, structural determination of sequence selectivity wasn't possible. 2D NMR analysis confirms the formation of some ROTERP terpolymer links, with proton signals in the 3.00–3.10 ppm range correlating to trithiocarbonate groups at around 220 ppm. Nevertheless, significant thioester formation is observed in the ^{13}C NMR, indicating poor sequence selectivity. GPC analysis shows a low apparent molar mass (M_w = 3 kg/mol, $Đ$ = 1.5), suggesting poor polymerization control, likely due to transesterification side reactions. DSC reveals the material is amorphous with a T_g = 37 °C and a decomposition onset at $T_{d,5\%}$ = 211 °C.

Phenyl glycidyl ether (PGE, run #7) achieved 99 % PTA conversion after 20 h, yielding a polymer with 79 % polymer selectivity and 84 % sequence selectivity. The polymer has an apparent M_w = 25 kg/mol ($Đ$ = 1.9), T_g = 37 °C, and $T_{d,5\%}$ = 250 °C. Its aliphatic analogue, ethyl glycidyl ether (EGE, run #8), improved polymer selectivity to 97 %, albeit at the cost of reduced sequence selectivity (79 %). The resulting amorphous polymer had an M_w = 26 kg/mol ($Đ$ = 1.6), T_g = 9 °C, and $T_{d,5\%}$ = 241 °C. These results show that glycidyl ethers—of which a wide variety of versions with functional substituents exist (see below)—are well tolerated in the ROTERP process.

Glycidyl ethers are synthesized from epichlorohydrin (ECH, run #9), an epoxide with widespread industrial relevance. ECH reached 90 % PTA conversion after 15 h, with 92 % polymer selectivity and 91 % sequence selectivity, producing a polymer with M_w = 24 kg/mol ($Đ$ = 1.9). DSC analysis tentatively supports the selectivity, showing a distinct, unbroadened T_g at 54 °C, with no additional transitions indicative of branching or cross-linking. This is somewhat surprising, as the electrophilic RCH_2Cl group in ECH and its polymers could be expected to undergo S_N2 attack by the nucleophilic sulfur chain ends—an issue observed in related polymerizations [49]. ^{1}H NMR reveals minor sequence errors from co-occurring ROCOP, particularly signals between 3.55 and 3.47 ppm that correlate with a thioester carbon at 193 ppm in the HMBC. Furthermore, the presence of RCH_2Cl groups is confirmed via HSQC correlation of the CH_2 resonance at 3.79 ppm with a 45 ppm signal, typical of halogen-adjacent carbons. No polymer links from side reactions of the chain end with the RCH_2Cl groups could be observed.

Next, we investigated functional glycidyl ethers, beginning with (3-glycidyloxypropyl)trimethoxysilane (TMSE, run #10), which bears silyl functionality. After 45 min, the reaction viscosity increased drastically, halting stirring. Crude ^{1}H NMR analysis indicated 84 % PTA conversion, 89 % polymer selectivity, and 88 % sequence selectivity. The resulting material had a T_g = –15 °C and $T_{d,5\%}$ = 255 °C. Moisture from ambient humidity slowly hydrolyzes the methoxy groups to silanols (–Si–OH), which undergo further condensation to form –Si–O–Si– linkages, creating an insoluble network [50]. Consequently, GPC analysis was not conducted to avoid instrument damage. However, the opportunity for crosslinking after ROTERP was leveraged to form shape-defined sulfur-containing silicones. A freshly precipitated polymer (from acidified methanol) was cast in a cylindrical mold and left under benchtop conditions for 3 days, followed by further storage in a humidified chamber (a desiccator containing water) and subsequent drying. The result was a cylindrical and brittle object. Gel fractions in DCM and THF, excellent solvents for the parent linear polymer, are 99 % confirming crosslinking. This procedure increased the T_g from –15 °C to –8 °C, and $T_{d,5\%}$ from 255 °C to 271 °C.

We then turned to vanillin glycidyl ether (VGE, run #11), synthesized from vanillin and epichlorohydrin. Although VGE is solid at room temperature, the ROTERP reaction temperature (80 °C) is above its melting point, enabling homogeneous polymerization. VGE reached 82 % PTA conversion after 22 h, producing 92 % polymer selectivity but a reduced sequence selectivity of 53 %. The ^{1}H NMR spectrum confirms that the aldehyde group remains intact, with a –CHO proton resonance

at 9.66 ppm. Despite moderate sequence control, the polymer displays favorable thermal properties (T_g = 81 °C, $T_{d,5\%}$ = 256 °C). However, its relatively low molar mass (M_w = 11 kg/mol) suggests limited control, likely due to side reactions such as transesterification [51].

Next, we investigated a functionalized carbazole epoxide (CE, run #12). Polymerization with PTA and CS_2 for 16 h gave 75 % PTA conversion and 70 % polymer selectivity. The isolated polymer had an M_w = 35 kg/mol, $Đ$ = 1.3, and exhibited an exceptional T_g = 163 °C ($T_{d,5\%}$ = 269 °C), which may be attributed to π–π interactions between carbazole units in the solid state.

Fluorinated monomers were also tested to evaluate their impact on polymer sequence and properties, particularly since fluorination is known to enhance thermal stability [52]. However, fluorinated ROCOP polymers remain scarcely explored [53–55]. 1,1,1-Trifluoro-2,3-epoxypropane (F-PO, run #13) was employed and reached 88 % PTA conversion, with a polymer selectivity of 56 %, and a molar mass of M_w = 25 kg/mol ($Đ$ = 1.6). DSC showed a T_g of 62 °C, while TGA recorded a $T_{d,5\%}$ of 314 °C—the highest thermal stability among all tested monomers. Compared to the non-fluorinated PO-based polymer, this reflects an increase of over 80 °C in thermal stability, highlighting the substantial effect of fluorination while maintaining catalytic performance and sequence selectivity. Phenylglycidylether with a C_6F_5 moiety (2,3-epoxypropyl pentafluorophenyl ether, F-PGE, run #14) reached 83 % PTA conversion after 5 h, with 93 % polymer selectivity and 87 % sequence selectivity. GPC analysis revealed a high M_w of 43 kg/mol, nearly double that of the non-fluorinated PGE under similar conditions. This increase may be attributed to inverse electron demand π–π stacking interactions involving the fluorinated aromatic ring, a phenomenon previously reported in ROCOP and potentially applicable here [54]. In contrast, thermal properties were only slightly improved: DSC revealed a T_g = 40 °C, and TGA showed $T_{d,5\%}$ = 255 °C, comparable to PGE. Fluorinated styrene oxide (2-(perfluorophenyl)oxirane, F-SO, run #15) showed poor reactivity, reaching only 10 % PTA conversion after 15 days. Similar to non-fluorinated SO, regioselectivity was not controlled due to regio-random epoxide ring-opening, making precise assessment of sequence selectivity difficult. GPC showed a M_w of 7 kg/mol. The polymer exhibited T_g = 90 °C and $T_{d,5\%}$ = 249 °C, both notably higher than the non-fluorinated counterpart. However, due to differences in molar mass, these thermal improvements cannot be unambiguously attributed to fluorination.

Finally, we explored difunctional bis-epoxides — an aliphatic version (DEO) and aromatic bisphenol A diglycidyl ether (BAGE) — to determine whether ROTERP could directly yield crosslinked networks. Each system was prepared using 1 equiv. LiOBn, 300 equiv. epoxide, 200 equiv. PTA, and 500 equiv. CS_2, with epoxide loading adjusted for the bifunctionality to encourage more uniform crosslinking. DEO yielded a soft, solid material within 1 h. After repeated purification via extraction, DSC revealed a T_g = –10 °C, and TGA a $T_{d,5\%}$ = 230 °C. BAGE-based polymer formed a stiffer material with a T_g = 84 °C and a T_d = 270 °C. However, as expected, neither material was soluble or thermally processable due to the crosslinked nature.

The ROTERP process introduces trithiocarbonate groups, which—due to the chemically soft lone pairs of sulfur—can interact with metals [56,57]. Moreover, it enables the incorporation of various functional epoxides into sulfur-containing polymers, presenting opportunities to tether these functionalities onto metal surfaces. To demonstrate this, gold nanoparticles (AuNPs) were functionalized with polymer ligands using a grafting-to approach, exploiting the affinity of trithiocarbonate groups for gold-nanoparticle surfaces (see ESI Section S 4) [58,59].

The polymer derived from vanillin glycidyl ether (VGE, run #11) was selected due to the presence of aldehyde groups on the vanillin moiety, which can participate in imine condensation. Prior to surface grafting, imine condensation was carried out between Rhodamine 110 and the polymer. This dye was selected as it can act as a fluorescent marker due to the fact that AuNPs are known to quench the fluorescence of nearby dye molecules in a distance-dependent manner [60,61].

Dynamic light scattering (DLS) measurements showed a modest increase in the hydrodynamic diameter of the AuNPs from 17 nm to 29 nm immediately after polymer grafting. This suggests the formation of a polymer shell via "wrapping" by the VGE-derived ROTERP terpolymer, which contains multiple trithiocarbonate groups along its main chain, as previously demonstrated for comparable systems [62]. After purification by centrifugation and re-dispersion, a further increase in hydrodynamic size to 139 nm was observed, indicating the formation of small nanoparticle agglomerates. Consistent with this, visible extinction spectroscopy revealed a pronounced red-shift of the plasmon resonance (see Fig. 5). This behavior is attributed to plasmon coupling interactions within the agglomerates which form during the performed purification of nanohybrids by centrifugation/re-dispersion [63]. This is likely a result of limited surface stabilization due to a relatively small polymer molar mass, "looped" multidentate binding to the nanoparticle surface, or a combination of both, leading to a comparably thin polymer shell (compare with DLS results above). However, extinction spectra recorded at various time points after purification showed no further shifts in the plasmon peak, indicating that the aggregation process did not proceed further, and a stable colloidal dispersion was obtained.

Imine functionalities are hydrolytically labile, enabling the potential for acid-triggered dye release. This was evaluated by analyzing the extinction spectra of the supernatant collected from functionalized AuNP dispersions after acid treatment. Upon the addition of HCl, extinction signals corresponding to Rhodamine were observed in the supernatant. Quantitative analysis based on dye extinction yielded an estimated released dye concentration of 0.7 μM. This corresponds to approximately 0.2 molecules of Rhodamine 110 chloride per nm^2 of nanoparticle surface area, calculated using a calibration curve obtained in the same solvent system.

Consistent with the known quenching effect of AuNPs, no fluorescence was observed in the dye–polymer–AuNP conjugate. However, fluorescence was restored upon acid addition, confirming dye release (see Fig. 6). As a control, AuNPs functionalized with thiol-terminated polystyrene pre-treated with Rhodamine in the same way showed no detectable dye release under identical acidic conditions. This demonstrates the system's unique capability to function as an efficient, pH-responsive nanoprobe.

3. Conclusions and Outlook

In conclusion, this study demonstrates the broad applicability of ring-opening terpolymerisation (ROTERP) for the synthesis of functional sulfur-containing polymers using a diverse range of epoxides. The method provides access to polymers containing poly(ester-*alt*-ester-*alt*-trithiocarbonate) linkages with tunable thermal and structural properties. From an environmental standpoint, the present synthetic route

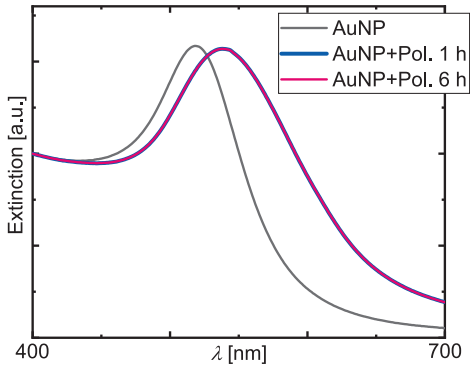

Fig. 5. Visible extinction spectra of citrate capped AuNPs (black trace) and polymer-functionalized AuNPs after 1 and 6 h (coloured traces) in a THF/DMF solvent mixture.

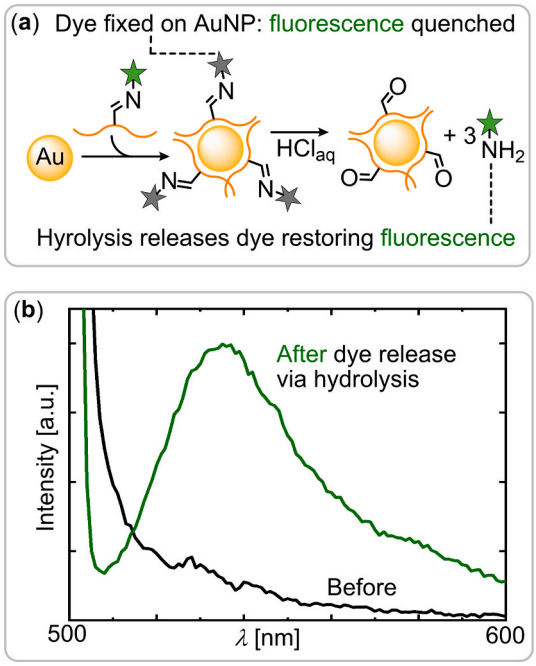

Fig. 6. (a) AuNP functionalisation and dye release methodology. (b) Fluorescence spectra of the AuNP solutions with polymer prior to and following acid addition.

cannot be classified as "green." The use of CS_2 and (halogenated) epoxides limits its sustainability. Nevertheless, the modularity of the ROTERP process and the wide commercial availability of its monomers make it a flexible and accessible platform for developing sulfur-containing polymers. However, side reactions are common and substantially impede the controllability of the methodology, particularly with respect to molecular weight predictability and polydispersity. These limitations are more pronounced for certain epoxides, resulting in only modest molecular weights under practical conditions. Importantly, the incorporation of sulfur centers enables downstream applications such as gold nanoparticle surface functionalization with built-in pH-responsive dye release. Overall, ROTERP represents a powerful and modular tool for designing advanced polymeric and nanomaterial systems with tailored functionalities.

4. Safety considerations

Both carbon disulfide and epoxides (especially ECH) are highly hazardous. These reagents are volatile, flammable, neurotoxic, sensitizing, and suspected carcinogens. All operations involving these reagents were conducted in a well-ventilated fume hood using appropriate personal protective gear. Reaction vessels were kept sealed under inert atmosphere as long as possible to minimize vapor exposure. Liquid and solid residues were quenched under basic conditions and collected in appropriate waste streams according to institutional hazardous-waste regulations.

Alex Plajer and Christian Rossner report financial support was provided by Chemical Industry Fund. Alex Plajer reports financial support was provided by German Research Foundation. Alex Plajer reports financial support was provided by Daimler and Benz Foundation. If there are other authors, they declare that they have no known competing financial interests or personal relationships that could have appeared to influence the work reported in this paper.

CRediT authorship contribution statement

Cesare Gallizioli: Investigation, Writing – original draft, Writing – review & editing. **Marina Sebastian:** Investigation, Writing – original draft, Writing – review & editing. **Malte Cornelsen:** Investigation. **Christian Rossner:** Conceptualization, Investigation, Resources, Supervision, Writing – original draft, Writing – review & editing. **Alex J. Plajer:** Conceptualization.

Declaration of competing interest

The authors declare that they have no known competing financial interests or personal relationships that could have appeared to influence the work reported in this paper.

Acknowledgements

We thank the "Fonds der Chemischen Industrie" (Liebig fellowships to CR and AJP) and the "Daimler and Benz Foundation" (personal scholarship for A. J. P) as well as the "Deutsche Forschungsgemeinschaft" (project number 542928411, CRC 1585 project number 492723217 for subproject SP01) for financial support. Andreas Fery is thanked for helpful discussions. Juan Guevara and Nina Nestmann are thanked for experimental support.

Data availability

Data will be made available on request.

References

[1] T.-J. Yue, W.-M. Ren, X.-B. Lu, Copolymerization involving sulfur-containing monomers, Chem. Rev. 123 (2023) 14038–14083, https://doi.org/10.1021/acs.chemrev.3c00437.
[2] H. Mutlu, E.B. Ceper, X. Li, J. Yang, W. Dong, M.M. Ozmen, P. Theato, Sulfur chemistry in polymer and materials science, Macromol. Rapid Commun. 40 (2019) 1800650, https://doi.org/10.1002/marc.201800650.
[3] N.M. Bingham, Z. Abousalman-Rezvani, K. Collins, P.J. Roth, Thiocarbonyl chemistry in polymer science, Polym. Chem. 13 (2022) 2880–2901, https://doi.org/10.1039/D2PY00050D.
[4] T. Lee, P.T. Dirlam, J.T. Njardarson, R.S. Glass, J. Pyun, Polymerizations with elemental sulfur: from petroleum refining to polymeric materials, J. Am. Chem. Soc. 144 (2022) 5–22, https://doi.org/10.1021/jacs.1c09329.
[5] S. Zheng, S.-S. Chen, Y.-Y. Li, M. Liao, X. Liang, K. Li, X. Li, J. Hu, D.-F. Chen, Monomer design enables mechanistic mapping of anionic ring-opening polymerization of aromatic thionolactones, Angew. Chem. Int. Ed. 64 (2025) e202500581, https://doi.org/10.1002/anie.202500581.
[6] S.P. Keyser, B.D. Fairbanks, J.T. Kamps, C.N. Bowman, Preparation of degradable polymers containing tunable ratios of dithioacetals and disulfides via mixed mode polymerization, Angew. Chem. Int. Ed. 64 (2025) e202515269, https://doi.org/10.1002/anie.202515269.
[7] A.W. Woodhouse, B. Pektas, C.M.Q. Le, J.A. Garden, H. Mutlu, Lauric diacid-derived sulfur-decorated functional polymers displaying programmable thermal and unconventional luminescence properties by simple thionation, Macromol. Rapid Commun. (2025) e00056, https://doi.org/10.1002/marc.202500056.
[8] Y. Wang, Y. Zhu, W. Lv, X. Wang, Y. Tao, Tough while recyclable plastics enabled by monothiodilactone monomers, J. Am. Chem. Soc. 145 (2023) 1877–1885, https://doi.org/10.1021/jacs.2c11502.
[9] W. Pei, Y. Liu, Q. Yan, K. Yuan, S. Li, Y. Shen, Z. Li, Crystallization/precipitation driven nonequilibrium ring-opening polymerization of thiovalerolactone toward closed-loop recyclable polythioester with excellent barrier properties, Angew. Chem. Int. Ed. 64 (2025) e202505104, https://doi.org/10.1002/anie.202505104.
[10] A. Calderón-Díaz, L. Ordner, M.G. Bernbeck, M. Palesati, M. Weber, N. Stingelin, W.R. Gutekunst, Topochemical ring-opening polymerization of an oxathianethione, J. Am. Chem. Soc. 147 (2025) 21331–21338, https://doi.org/10.1021/jacs.5c06180.
[11] Y. Xiao, T.-J. Yue, B.-H. Ren, W.-M. Ren, X.-B. Lu, Isotactic-rich polythioethers synthesized from asymmetric ring-opening polymerization of racemic terminal thiiranes, ACS Catal. 13 (2023) 16215–16221, https://doi.org/10.1021/acscatal.3c04332.
[12] L. Zhou, L.T. Reilly, C. Shi, E.C. Quinn, E.-Y.-X. Chen, Proton-triggered topological transformation in superbase-mediated selective polymerization enables access to ultrahigh-molar-mass cyclic polymers, Nat. Chem. 16 (2024) 1357–1365, https://doi.org/10.1038/s41557-024-01511-2.
[13] Y. Zhu, Y. Tao, Stereoselective ring-opening polymerization of s-carboxyanhydrides using salen aluminum catalysts: a route to high-isotactic functionalized polythioesters, Angew. Chem. Int. Ed. 63 (2024) e202317305, https://doi.org/10.1002/anie.202317305.
[14] B.R. Manjunatha, C. Gallizioli, C. Fornacon-Wood, J. Stephan, M.R. Stühler, A. J. Plajer, Sequence control in sulphur-containing ring-opening co- and

terpolymerisations, Angew. Chem. Int. Ed. 64 (2025) e202507243, https://doi.org/10.1002/anie.202507243.
[15] J.-Z. Zhao, T.-J. Yue, B.-H. Ren, Y.-X. Ma, X.-B. Lu, W.-M. Ren, Chemically recyclable poly(tetrathioorthocarbonate)s: combining high refractive index and abbe number, J. Am. Chem. Soc. 147 (2025) 19762–19769, https://doi.org/10.1021/jacs.5c03424.
[16] J. Stephan, J.L. Olmedo-Martínez, C. Fornacon-Wood, M.R. Stühler, M. Dimde, D. Braatz, R. Langer, A.J. Müller, H. Schmalz, A.J. Plajer, Easy Synthetic access to high-melting sulfurated copolymers and their self-assembling diblock copolymers from phenylisothiocyanate and oxetane, Angew. Chem. Int. Ed. 63 (2024) e202405047, https://doi.org/10.1002/anie.202405047.
[17] M.R. Stühler, M. Kreische, C. Fornacon-Wood, S.M. Rupf, R. Langer, A.J. Plajer, Monomer centred selectivity guidelines for sulfurated ring-opening copolymerisations, Chem. Sci. 15 (2024) 19029–19036, https://doi.org/10.1039/D4SC05858E.
[18] B.R. Manjunatha, K.S. Marcus, R.M. Gomila, A. Frontera, A.J. Plajer, Harnessing borane-potassium cooperativity for sulfurated ring-opening copolymerisation, Green Chem. 27 (2025) 3494–3502, https://doi.org/10.1039/D4GC05665E.
[19] J. Stephan, M.R. Stühler, S.M. Rupf, S. Neale, A.J. Plajer, Mechanistic mapping of (CS_2/CO_2)/epoxide copolymerization catalysis leads to terpolymers with improved degradability, Cell Rep. Phys. Sci. (2023) 101510, https://doi.org/10.1016/j.xcrp.2023.101510.
[20] M. Sengoden, G.A. Bhat, D.J. Darensbourg, Explorations into the sustainable synthesis of cyclic and polymeric carbonates and thiocarbonates from eugenol-derived monomers and their reactions with CO2, COS, or CS2, Green Chem. 24 (2022) 2535–2541, https://doi.org/10.1039/D2GC00327A.
[21] C. Fornacon-Wood, M.R. Stühler, C. Gallizioli, B.R. Manjunatha, V. Wachtendorf, B. Schartel, A.J. Plajer, Precise construction of weather-sensitive poly(ester-alt-thioesters) from phthalic thioanhydride and oxetane, Chem. Commun. 59 (2023) 11353–11356, https://doi.org/10.1039/D3CC03315E.
[22] B.R. Manjunatha, M.R. Stühler, L. Quick, A.J. Plajer, Improved access to polythioesters by heterobimetallic aluminium catalysis, Chem. Commun. 60 (2024) 4541–4544, https://doi.org/10.1039/D4CC00811A.
[23] X. Yue, W. Guo, X. Liu, Q. Yu, X. Lu, C. Zhang, X. Zhang, Organocatalyzed copolymerization of CO, Se, and oxetane: O/Se exchange reaction determining chain structure, Angew. Chem. Int. Ed. 137 (2025) e202504180, https://doi.org/10.1002/ange.202504180.
[24] G. Feng, X. Feng, X. Liu, C. Zhang, X. Zhang, Organocatalytic synthesis of poly (thiocarbonate) from xylose and carbonyl sulfide, Macromolecules 57 (2024) 3757–3764, https://doi.org/10.1021/acs.macromol.4c00303.
[25] W.-D. Chu, S.-Y. Dan, J. Zhan, B. Chen, J. Xian, C.-M. Wang, Q.-Z. Liu, J. Wu, C.-A. Fan, Facile synthesis of recyclable polythioimidocarbonates via aromatization-driven alternating copolymerization of para -quinone methide and isothiocyanates, Chem. Sci. 16 (2025) 5493–5502, https://doi.org/10.1039/D5SC00050E.
[26] D.K. Tran, A.N. Braaksma, A.M. Andras, S.K. Boopathi, D.J. Darensbourg, K. L. Wooley, Structural metamorphoses of d-xylose oxetane- and carbonyl sulfide-based polymers in situ during ring-opening copolymerizations, J. Am. Chem. Soc. 145 (2023) 18560–18567, https://doi.org/10.1021/jacs.3c05529.
[27] X.-F. Zhu, G.-W. Yang, R. Xie, G.-P. Wu, One-pot construction of sulfur-rich thermoplastic elastomers enabled by metal-free self-switchable catalysis and air-assisted coupling, Angew. Chem. Int. Ed. 61 (2022) e202115189, https://doi.org/10.1002/anie.202115189.
[28] H.-T. Zhang, M.-X. Niu, Q. Zhang, C.-Y. Hu, X. Pang, Facile synthesis of polyisothioureas via alternating copolymerization of aziridines and isothiocayanates, Chin. J. Polym. Sci. 42 (2024) 292–298, https://doi.org/10.1007/s10118-023-3048-6.
[29] G. Feng, X. Feng, X. Liu, W. Guo, C. Zhang, X. Zhang, Metal-free alternating copolymerization of CS_2 and oxetane, Macromolecules 56 (2023) 6798–6805, https://doi.org/10.1021/acs.macromol.3c01300.
[30] I. Yamamoto, S. Muranaka, K. Hirose, T. Ema, Terpolymerization of oxetane, CO2, and isothiocyanates with bifunctional catalysts: synthesis and degradability of poly (thioimidocarbonate-trimethylene carbonate)s, ACS Appl. Polym. Mater. 7 (2025) 5116–5126, https://doi.org/10.1021/acsapm.5c00415.
[31] S. Rupf, P. Pröhm, A.J. Plajer, Lithium achieves sequence selective ring-opening terpolymerisation (ROTERP) of ternary monomer mixtures, Chem. Sci. 13 (2022) 6355–6365, https://doi.org/10.1039/D2SC01776H.
[32] P. Deglmann, S. Machleit, C. Gallizioli, S.M. Rupf, A.J. Plajer, Lithium catalysed sequence selective ring opening terpolymerisation: a mechanistic study, Cat. Sci. Tech. 13 (2023) 2937–2945, https://doi.org/10.1039/D3CY00301A.
[33] A.J. Plajer, Sequence selective ring-opening terpolymerisation facilitates higher order switchable catalysis, ChemCatChem 14 (2022) e202200867, https://doi.org/10.1002/cctc.202200867.
[34] L.-Y. Wang, G.-G. Gu, T.-J. Yue, W.-M. Ren, X.-B. Lu, Semiaromatic poly(thioester) from the copolymerization of phthalic thioanhydride and epoxide: synthesis, structure, and properties, Macromolecules 52 (2019) 2439–2445, https://doi.org/10.1021/acs.macromol.9b00073.
[35] L.-Y. Wang, G.-G. Gu, B.-H. Ren, T.-J. Yue, X.-B. Lu, W.-M. Ren, Intramolecularly cooperative catalysis for copolymerization of cyclic thioanhydrides and epoxides: a dual activation strategy to well-defined polythioesters, ACS Catal. 10 (2020) 6635–6644, https://doi.org/10.1021/acscatal.0c00906.
[36] J. Qin, Z. Xu, H. Wang, X. Tang, Cyclic poly(thioester amide)s via ring-opening copolymerization of aziridines and phthalic thioanhydride: mechanistic insights and enhanced properties for sustainable materials, Macromolecules 58 (2025) 7686–7696, https://doi.org/10.1021/acs.macromol.5c00511.
[37] K. Han, M. Wang, Z. Ding, Z. Zhou, B. Wang, Y. Li, Cyclic thioanhydride/episulfide copolymerizations catalyzed by bipyridine-bisphenolate aluminum/onium pair: approach to structurally and functionally diverse poly(thioester)s, Polym. Chem. 15 (2024) 2502–2512, https://doi.org/10.1039/D4PY00479E.
[38] X.-L. Chen, B. Wang, D.-P. Song, L. Pan, Y.-S. Li, One-step synthesis of sequence-controlled polyester-block-poly(ester-alt-thioester) by chemoselective multicomponent polymerization, Macromolecules 55 (2022) 1153–1164, https://doi.org/10.1021/acs.macromol.1c02303.
[39] J. Diebler, H. Komber, L. Häußler, A. Lederer, T. Werner, Alkoxide-initiated regioselective coupling of carbon disulfide and terminal epoxides for the synthesis of strongly alternating copolymers, Macromolecules 49 (2016) 4723–4731, https://doi.org/10.1021/acs.macromol.6b00728.
[40] D. Silbernagl, H. Sturm, A.J. Plajer, Thioanhydride/isothiocyanate/epoxide ring-opening terpolymerisation: sequence selective enchainment of monomer mixtures and switchable catalysis, Polym. Chem. 13 (2022) 3981–3985, https://doi.org/10.1039/D2PY00629D.
[41] C. Gallizioli, D. Battke, H. Schlaad, P. Deglmann, A.J. Plajer, Ring-opening terpolymerisation of elemental sulfur waste with propylene oxide and carbon disulfide via lithium catalysis, Angew. Chem. Int. Ed. 63 (2024) e202319810, https://doi.org/10.1002/anie.202319810.
[42] C. Gallizioli, P. Deglmann, A.J. Plajer, Kinetically enhanced access to a dynamic polyester platform via sequence selective terpolymerisation of elemental sulphur, Angew. Chem. Int. Ed. 64 (2025) e202501337, https://doi.org/10.1002/anie.202501337.
[43] J. Herzberger, K. Niederer, H. Pohlit, J. Seiwert, M. Worm, F.R. Wurm, H. Frey, Polymerization of ethylene oxide, propylene oxide, and other alkylene oxides: synthesis, novel polymer architectures, and bioconjugation, Chem. Rev. 116 (2016) 2170–2243, https://doi.org/10.1021/acs.chemrev.5b00441.
[44] A. Sirin-Sariaslan, S. Naumann, Chiral diboranes as catalysts for the stereoselective organopolymerization of epoxides, Chem. Sci. 13 (2022) 10939–10943, https://doi.org/10.1039/D2SC03977J.
[45] J. Park, A. Kim, B.-S. Kim, Anionic ring-opening polymerization of functional epoxide monomers in the solid state, Nat. Commun. 14 (2023) 5855, https://doi.org/10.1038/s41467-023-41576-0.
[46] M. Sugiyama, R. Suzuki, H. Ayakawa, T. Gao, F. Li, T. Yamamoto, T. Isono, T. Satoh, Ring-opening alternating copolymerization of cyclic anhydrides and isobutylene oxide using organobase catalysts, Polym. J. (2025) 1–11, https://doi.org/10.1038/s41428-025-01087-9.
[47] A.J. Plajer, C.K. Williams, Heterotrimetallic carbon dioxide copolymerization and switchable catalysts: sodium is the key to high activity and unusual selectivity, Angew. Chem. Int. Ed. 60 (2021) 13372–13379, https://doi.org/10.1002/anie.202101180.
[48] S. Zhao, C.-K. Xu, Y. Gong, G.-W. Yang, G.-P. Wu, Copolymerization of styrene oxide with CO2 via modular optimization of bifunctional organoborane catalysts, Eur. Polym. J. (2025) 113912, https://doi.org/10.1016/j.eurpolymj.2025.113912.
[49] T.-J. Yue, G.A. Bhat, W.-J. Zhang, W.-M. Ren, X.-B. Lu, D.J. Darensbourg, Facile synthesis of well-defined branched sulfur-containing copolymers: one-pot copolymerization of carbonyl sulfide and epoxide, Angew. Chem. Int. Ed. 132 (2020) 13735–13739, https://doi.org/10.1002/ange.202005806.
[50] D. Huebner, V. Koch, B. Ebeling, J. Mechau, J.E. Steinhoff, P. Vana, Comparison of monomethoxy-, dimethoxy-, and trimethoxysilane anchor groups for surface-initiated RAFT polymerization from silica surfaces, J. Polym. Sci. 53 (2015) 103–113, https://doi.org/10.1002/pola.27454.
[51] J. Xu, P. Zhang, Y. Yuan, N. Hadjichristidis, Elucidation of the alternating copolymerization mechanism of epoxides or aziridines with cyclic anhydrides in the presence of halide salts, Angew. Chem. Int. Ed. 62 (2024) e202218891, https://doi.org/10.1002/anie.202218891.
[52] B. Ameduri, Fluoropolymers: the right material for the right applications, Chem Eur J 24 (2018) 18830–18841, https://doi.org/10.1002/chem.201802708.
[53] C. Fornacon-Wood, M.R. Stühler, A. Millanvois, L. Steiner, C. Weimann, D. Silbernagl, H. Sturm, B. Paulus, A.J. Plajer, Fluoride recovery in degradable fluorinated polyesters, Chem. Commun. 60 (2024) 7479–7482, https://doi.org/10.1039/D4CC02513J.
[54] C. Fornacon-Wood, L. Steiner, C. Xu, B. Paulus, A.J. Plajer, in revision.
[55] C. Zhao, G. He, T. Chen, H. Li, J. Zhao, Precision organocatalytic synthesis of fluoropolyesters with enhanced degradability and ionic conductivity, Macromolecules 58 (2025) 1630–1641, https://doi.org/10.1021/acs.macromol.4c03117.
[56] J. Stephan, M.R. Stühler, C. Fornacon-Wood, M. Dimde, K. Ludwig, H. Sturm, J. L. Olmedo-Martínez, A.J. Müller, A.J. Plajer, Sulfur-containing block polymers from ring-opening copolymerization: coordinative encapsulants for transition metals, Polym. Chem. 16 (2025) 1003–1009, https://doi.org/10.1039/D4PY01415D.
[57] C.-A. Fustin, A.-S. Duwez, Dithioesters and trithiocarbonates monolayers on gold, J. Electron Spectrosc. 172 (2009) 104–106, https://doi.org/10.1016/j.elspec.2009.03.009.
[58] C. Rossner, Polymer-grafted gold colloids and supracolloids: from mechanisms of formation to dynamic soft matter, Macromol. Rapid Commun. 46 (2025) 2400851, https://doi.org/10.1002/marc.202400851.
[59] C. Rossner, V. Roddatis, S. Lopatin, P. Vana, Functionalization of planet–satellite nanostructures revealed by nanoscopic localization of distinct macromolecular species, Macromol. Rapid Commun. 37 (2016) 1742–1747, https://doi.org/10.1002/marc.201600480.
[60] C. Cepraga, A. Favier, F. Lerouge, P. Alcouffe, C. Chamignon, P.-H. Lanoë, C. Monnereau, S. Marotte, E.B. Daoud, J. Marvel, Y. Leverrier, C. Andraud, S. Parola, M.-T. Charreyre, Fluorescent gold nanoparticles with chain-end grafted RAFT copolymers: influence of the polymer molecular weight and type of

chromophore, Polym. Chem. 7 (2016) 6812–6825, https://doi.org/10.1039/C6PY01625A.
[61] P. Anger, P. Bharadwaj, L. Novotny, Enhancement and quenching of single-molecule fluorescence, Phys. Rev. Lett. 96 (2006) 113002, https://doi.org/10.1103/PhysRevLett.96.113002.
[62] B. Ebeling, P. Vana, RAFT-polymers with single and multiple trithiocarbonate groups as uniform gold-nanoparticle coatings, Macromolecules 46 (2013) 4862–4871, https://doi.org/10.1021/ma4008626.
[63] C. Rossner, T.A.F. König, A. Fery, Plasmonic properties of colloidal assemblies, Adv. Opt. Mater. 9 (2021) 2001869, https://doi.org/10.1002/adom.202001869.